Controlling chaos to unstable periodic orbits and equilibrium state solutions for the coupled dynamos system*

Wu Shu-Hua(吴淑花)[a)b)†], Hao Jian-Hong(郝建红)[a)], and Xu Hai-Bo(许海波)[c)]

[a)] *School of Electric and Electronic Engineering, North China Electric Power University, Beijing* 102206, *China*
[b)] *Department of Physics and Electrical Information Engineering, Shijiazhuang Normal College, Shijiazhuang* 050035, *China*
[c)] *Institute of Applied Physics and Computational Mathematics, Beijing* 100088, *China*

(Received 3 June 2009; revised manuscript received 28 July 2009)

In the case where the knowledge of goal states is not known, the controllers are constructed to stabilize unstable steady states for a coupled dynamos system. A delayed feedback control technique is used to suppress chaos to unstable focuses and unstable periodic orbits. To overcome the topological limitation that the saddle-type steady state cannot be stabilized, an adaptive control based on LaSalle's invariance principle is used to control chaos to unstable equilibrium (i.e. saddle point, focus, node, etc.). The control technique does not require any computer analysis of the system dynamics, and it operates without needing to know any explicit knowledge of the desired steady-state position.

Keywords: coupled dynamos system, delayed feedback control, adaptive control, controlling chaos

PACC: 0545, 0555

1. Introduction

The problem of controlling chaos has attracted great interest among physicists over the past decade. The unique interest of physicists in this subject started with an observation that chaotic motion can be converted to any of a large number of periodic motions via the stabilization of unstable periodic orbits (UPOs) embedded in a chaotic attractor.[1] Various methods of controlling the chaotic system have been proposed in recent years. These methods can be divided into two broad categories: nonfeedback control and feedback control. To the feedback control, there are the Ott–Grebogi–Yorke (OGY) method, adaptive control, delayed feedback control (DFC), linear feedback control, nonlinear feedback control, alterable structure control, fuzzy control and so on. The nonfeedback control methods include weak periodic parametric perturbation, addition of weak periodic pulses, addition of weak noise signal, etc.[2−6] In Refs. [5] and [6], two control methods of periodic impulse and periodic pulses added have been well studied and applied successfully. Each method has its advantages and disadvantages. A suitable technique will ensure effectual chaos control.

Many studies have achieved the coupled dynamos system. In Ref. [7], the feedback (linear feedback and dual-feedback) techniques were used to control the dynamical system of coupled dynamos to unstable equilibrium points and limit cycles, and the numerical simulations showed that the controlling techniques were valid. Unfortunately, the knowledge of desired goal steady states for the chaotic system must be known accurately. In the present paper, the controlling idea in Ref. [7] is further extended. Without explicit knowledge of the steady-state position, controlling chaos to unstable periodic orbits and unstable equilibrium points can be realized by using DFC and adaptive control techniques. Numerical simulation results show the control process of the different methods.

2. System of coupled dynamos

The system of coupled dynamos is a nonlinear dynamical system which is capable of displaying chaotic behaviours. The system consists of two dynamos connected together so that the current generated by any one of them produces the magnetic field for another.[7−9] In Ref. [7], the coupled dynamos chaotic system is described by the following system of differ-

*Project supported by the Doctoral Foundation of North China Electric Power University (Grant No. kH0433) and the International Science and Technology Cooperation Program (Grant No. 2007DFA71250).
†Corresponding author. E-mail: wsh16888@126.com
© 2010 Chinese Physical Society and IOP Publishing Ltd

ential equations:

$$\begin{cases} \dot{x}_1 = -\mu x_1 + x_2(x_3 + \alpha), \\ \dot{x}_2 = -\mu x_2 + x_1(x_3 - \alpha), \\ \dot{x}_3 = x_3 - x_1 x_2, \end{cases} \tag{1}$$

where μ and α are positive control parameters. When $\mu > 1/2$, the divergence of the flow (1) is given by

$$\boldsymbol{\nabla} \cdot \boldsymbol{F} = \frac{\partial F_1}{\partial x_1} + \frac{\partial F_2}{\partial x_2} + \frac{\partial F_3}{\partial x_3} = -2\mu + 1 < 0,$$

where $\boldsymbol{F} = (F_1, F_2, F_3) = (-\mu x_1 + x_2(x_3 + \alpha), -\mu x_2 + x_1(x_3 - \alpha), x_3 - x_1 x_2)$.

Then, system (1) is a forced dissipative system similar to the famous Lorenz system, but not equivalent to it topologically. Thus solutions of system (1) are globally bounded for all $t \geq 0$ and continuously differentiable with respect to time. System (1) is invariable through the transformation of $(x_1, x_2, x_3) \to (-x_1, -x_2, x_3)$, from which it follows that the system (1) is symmetrical, with the x_3 axis regarded as its symmetrical axis.

2.1. Analysis of chaotic dynamics

In this section, the dynamics behaviour of the coupled dynamos system (1) is analysed at $\mu = 2$ and $\alpha = 3$. Figure 1(a) shows a three-dimensional image of the chaotic attractor for the coupled dynamos. Figure 1(b) shows the points of trajectories by section of $x_1 = 0$. These points on the Poincaré section form a pattern with a certain shape and self-similar structure. Figure 1(c) shows the continuous power spectrum of $x_3(t)$. Figure 1(d) shows a chaotic time series chart of $x_3(t)$.

Using the method of singular-value decomposition, as $t \to \infty$, three Lyapunov exponents of the system (1) are obtained to be $\lambda_1 = 0.4493$, $\lambda_2 = 0$, and $\lambda_3 = -3.4493$. According to Kaplan and Yorke speculation,[10] the Lyapunov dimension of chaos attractors of Eq. (1) can be derived to be

$$d_{\mathrm{e}} = j + \frac{1}{\lambda_{j+1}} \sum_{i=1}^{j} \lambda_i = 2 + \frac{\lambda_1 + \lambda_2}{|\lambda_3|} = 2.1303. \tag{2}$$

System (1) has a fractional dimension. Consequently, all the analysis above shows that the behaviour of the dynamical system (1) is chaotic at $\mu = 2$ and $\alpha = 3$.

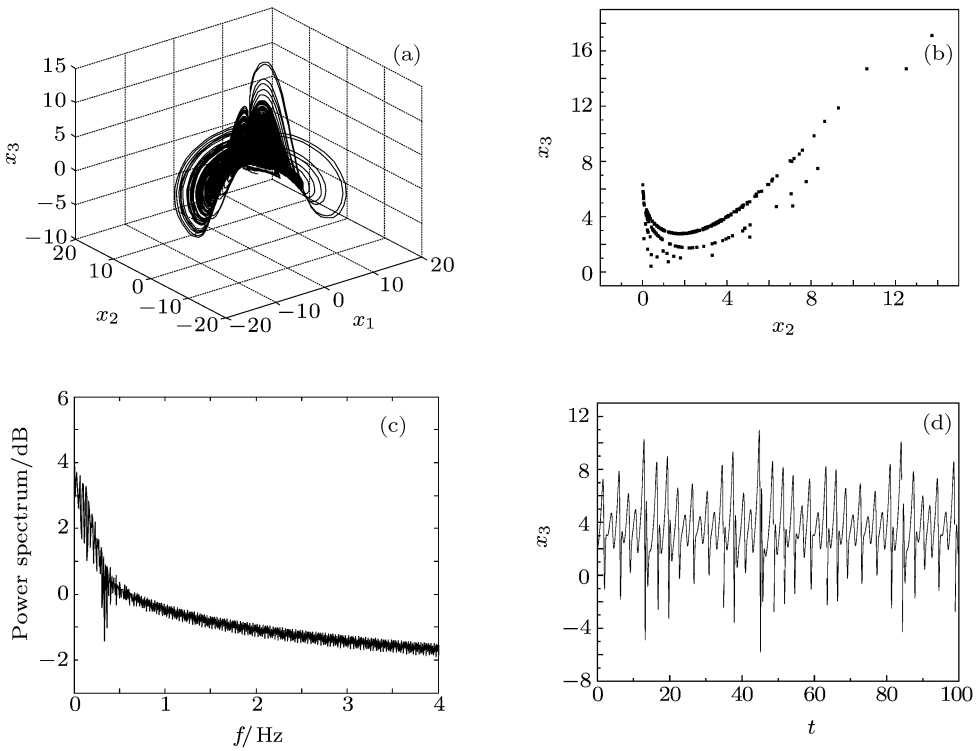


Fig. 1. Chaotic behaviours of system (1) at $\alpha = 3$ and $\mu = 2$. (a) chaotic attractor; (b) Poincaré section; (c) power spectrum of $x_3(t)$; (d) time series of $x_3(t)$.

2.2. Stability analysis of equilibrium states

Setting $\boldsymbol{F} = 0$, the mathematical model equations for this system (1) are

$$\begin{aligned} &-\mu x_1 + x_2(x_3 + \alpha) = 0, \\ &-\mu x_2 + x_1(x_3 - \alpha) = 0, \\ &x_3 - x_1 x_2 = 0. \end{aligned} \tag{3}$$

The equilibrium points of the system (1) are

$$\begin{aligned} &E_0 = (0,0,0), \quad E_1 = (-\beta_2, \beta_1, -\gamma), \\ &E_2 = (\beta_2, -\beta_1, -\gamma), \quad E_3 = (\beta_1, \beta_2, \gamma), \\ &E_4 = (-\beta_1, -\beta_2, \gamma), \end{aligned} \tag{4}$$

where $\beta_1 = \sqrt{\gamma(\gamma+\alpha)/\mu}$, $\beta_2 = \sqrt{\gamma(\gamma-\alpha)/\mu}$, and $\gamma = \sqrt{\alpha^2+\mu^2}$.

When the equilibrium state is expressed as $E(\bar{x}_1, \bar{x}_2, \bar{x}_3)$, the Jacobian of the linearized system about the equilibrium state E is

$$J(E) = \begin{bmatrix} -\mu & \bar{x}_3 + \alpha & \bar{x}_2 \\ \bar{x}_3 - \alpha & -\mu & \bar{x}_1 \\ -\bar{x}_2 & -\bar{x}_1 & 1 \end{bmatrix}.$$

The equation with the eigenvalues is

$$\begin{aligned} &\lambda^3 + (2\mu - 1)\lambda^2 + (\alpha^2 + \mu^2 - 2\mu + \bar{x}_1^2 + \bar{x}_2^2 - \bar{x}_3^2)\lambda \\ &+ (\mu\bar{x}_1^2 + \mu\bar{x}_2^2 + \bar{x}_3^2 + 2\bar{x}_1\bar{x}_2\bar{x}_3 - \alpha^2 - \mu^2) = 0. \end{aligned}$$

Lemma 1 As $\mu = 2$ and $\alpha = 3$, the equilibrium solution $E_0 = (0,0,0)$ of the uncontrolled system (1) is an unstable saddle point.

Proof As $\mu = 2$ and $\alpha = 3$, the eigenvalues of the first equilibrium state E_0 are $\lambda_1 = 1$, $\lambda_2 = -2 + 3\,\mathrm{i}$ and $\lambda_3 = -2 - 3\,\mathrm{i}$. Since λ_1 is a positive real number, λ_2 and λ_3 are a pair of complex conjugate eigenvalues with negative real parts, it follows that E_0 is an unstable saddle point.

Lemma 2 As $\mu = 2$ and $\alpha = 3$, these equilibrium solutions ($E_1 \sim E_4$) of the uncontrolled system (1) are unstable focuses.

Proof As $\mu = 2$ and $\alpha = 3$, the eigenvalues of the equilibrium solution $E_1 = (-\beta_2, \beta_1, -\gamma)$ are $\lambda_1 = -4.0$, $\lambda_2 = 0.50 + 3.5706\,\mathrm{i}$, and $\lambda_3 = 0.50 - 3.5706\,\mathrm{i}$. Since λ_1 is a negative real number, λ_2 and λ_3 are a pair of complex conjugate eigenvalues with positive real parts, it follows that E_1 is an unstable focus. Similar calculation shows that the others ($E_2 \sim E_4$) with the same eigenvalues are also unstable focuses for system (1).

Obviously, these unstable equilibrium states ($E_1 \sim E_4$) with uniform stability are symmetrical. The chaotic attractor of Eq. (1) is not only common to a low-dimensional chaotic system, but also has more complex folding and stretchable trajectories, thereby showing Eq. (1) to be more locally unstable than the low-dimensional chaotic system. The coupled dynamos system has five equilibrium points, but the Lorenz system has only three. Figure 1(a) shows that the unstable saddle point E_0 is in the middle of the chaotic attractor which takes the x_3 axis as a symmetrical axis. It is surrounded by four circular regions around an unstable focus separately, forming a spiral chaotic multi-attractor. Therefore, it is totally different from the Lorenz system, and its complexity will greatly increase the difficulty in controlling the chaos.

3. Controlling chaos

In this section, the chaos of the dynamical system (1) is controlled to unstable equilibrium solutions and UP0s. Delayed feedback control method and adaptive control method are used to achieve this goal.

3.1. Delayed feedback control method

DFC method is indeed capable of stabilizing not only UPOs, but also unstable steady states. It involves a control signal formed from the difference between the current state of the system and the state of the system delayed by one period of the UPOs, so that the control signal vanishes when the stabilization of the desired orbit is attained. The proposed delayed feedback controller $D(t)$ with time consists of the current state $x(t)$ and the delayed state $x(t-\tau)$ in the form of $D(t) = x(t) - x(t-\tau)$, where $D(t)$ is the $i \times i$ matrix and τ is the delay time which is the adjusted parameter. In the controlled system, the controller $D(t)$ converges to zero when the trajectories converge to one of UPOs (or equilibrium solutions) with periodic τ, then the controlled and uncontrolled systems have the same solutions naturally.

The DFC method is applied to system (1). Generally, the dimension of the proposed controller is reduced. In this case, $D(t)$ only disturbs the third equation of system (1), and the result of controlled system

has the following forms:

$$\begin{pmatrix} \dot{x}_1 \\ \dot{x}_2 \\ \dot{x}_3 \end{pmatrix} = \begin{pmatrix} -\mu x_1 + x_2(x_3 + \alpha) \\ -\mu x_2 + x_1(x_3 - \alpha) \\ x_3 - x_1 x_2 \end{pmatrix} - KD(t) \begin{pmatrix} 0 \\ 0 \\ 1 \end{pmatrix}, \tag{5}$$

hence,

$$D(t) = x_3(t) - x_3(t - \tau), \tag{6}$$

where K is the feedback gain. Experimentally, stabilization is achieved by fitting two parameters τ and K in such a way as to minimize the amplitude of the perturbation $KD(t)$. The method is not very sensitive to the variation of K. If τ is chosen correctly, there exists a finite interval of values of K achieving stabilization.[11] In the present paper, K is set to be 0.7.

However, an experimental fitting of the delay time τ is more complicated and requires a very thorough adjustment, because the amplitude of the perturbation has a resonance-type dependence on τ with pronounced minima at τ coinciding with the periods of the UPOs. To provide the small amplitude of the perturbation, the delay time must be fitted to be as close as possible to the period T_k of the desired UPO. The search for the correct value of τ is particularly difficult for autonomous systems, because the periods of their UPOs are *a priori* unknown.

The correct value of τ can be found by observing the variation of $D(t)$ with τ. For the changes in the parameter of τ, the value of $D(t)$ is obtained by averaging over 6000 calculation results or more to eliminate 'butterfly effect'. In order to avoid neutralizing effect of the $D(t)$ deviating from zero, the variation of $D^2(t)$ with τ is studied here. At the same time, $D^2(t)$ is square mean of $D(t)$ except for the initial transient data.[12] The correct value τ can be chosen arbitrarily when $D^2(t) \approx 0$. Figure 2 shows the variation of

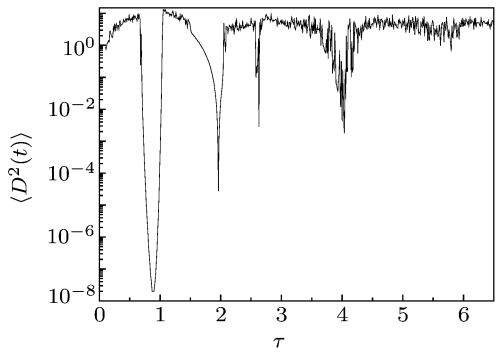


Fig. 2. Variation of $\langle D^2(t) \rangle$ with τ.

$D^2(t)$ with τ in controlled systems (5) and (6). When τ is chosen to be one of the following values: 0.9, 1.96, 2.62, 4.04, the value of $D^2(t)$ will be on the verge of zero. Sympathetic vibration occurs between delayed feedback and inherent UPO (or unstable equilibrium state), and the chaotic system (1) is stabilized to UPO or unstable fixed point accurately.

The controlled system of ordinary differential equation (5) and the control system (6) are integrated by using the fourth-order Runge–Kutta method with time steps of 0.01. The parameters μ and α are taken to be 2 and 3 respectively, i.e. $\mu = 2$ and $\alpha = 3$, to ensure the existence of chaos in the absence of the control. The $K = 0.7$, $\tau = 0.9$ and the initial conditions $(x_1, x_2, x_3)_{t=0} = (-1, -1, -1)$ are chosen. The unstable focus $E_1(-1.045, 3.451, -3.606)$ of system (5) is stabilized when the control is activated at $t = 70$. Figure 3 shows the behaviours of the states x_1, x_2 and x_3 of system (5) and the controller $D(t)$ evolution with time. The numerical simulations show a successful stabilization of the equilibrium state with an asymptotically vanishing perturbation. Choosing a different initial value, other unstable focuses (E_2, E_3 and E_4) are stabilized. As $\tau = 2.62$ and $(x_1, x_2, x_3)_{t=0} = (-1, 1, 1)$, equation (5) is stabilized at $E_4(-3.451, -1.045, 3.606)$ when the control is activated at $t = 70$. Figure 4 shows the behaviours of the states x_1, x_2 and x_3 of system (5) and the controller $D(t)$ evolution with time. In the same way, changing the initial value, other focuses are stabilized. As $\tau = 1.96$ and $(x_1, x_2, x_3)_{t=0} = (-1, -1, 1)$, the trajectories converge to period-1 orbit. The results of stabilizing period-1 orbit are presented in Figs. 5(a)–5(c). The perturbation before and after switching on the control is presented in Fig. 5(d). The amplitude of the perturbation gradually decreases and the desired UPO becomes stable. Changing the initial value, the trajectories will converge to another period-1 orbit and the two period-1 orbits are symmetrical with respect to x_3 axis. As $\tau = 4.04$, the trajectories converge to period-2 orbit. The results of stabilizing period-2 orbit are presented in Figs. 6(a)–6(c). The perturbation before and after switching on the control is presented in Fig. 6(d). Similarly, taking a different initial state, the trajectories will converge to another period-2 orbit. Experimentally, no matter how to select the values of K and τ, system (5) cannot be controlled to the unstable saddle point E_0.

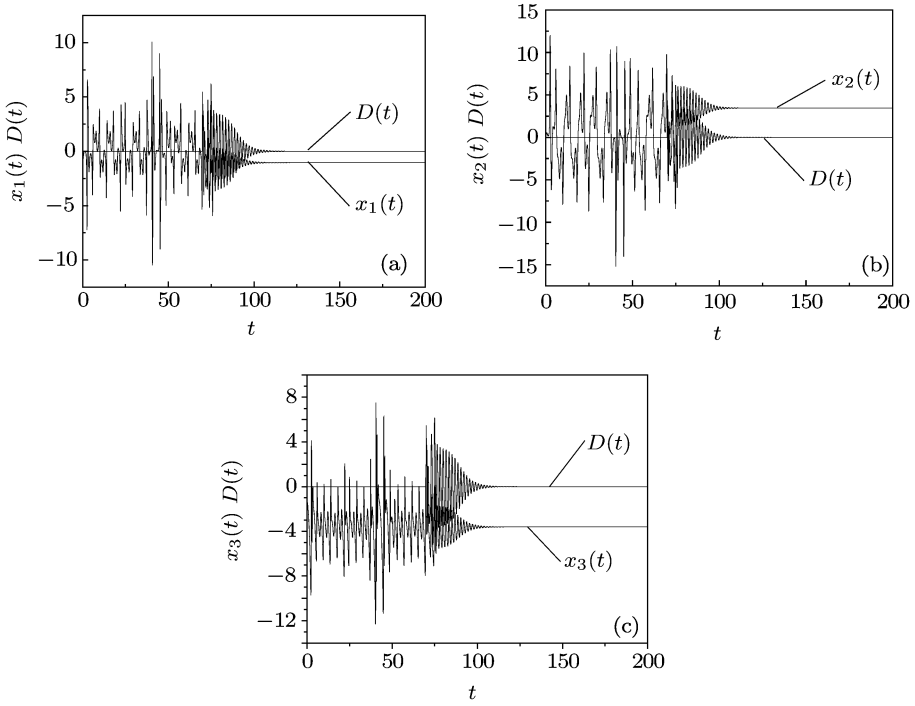


Fig. 3. The states of the controlled system (5) and the control system (6) response for $\tau = 0.9$ and $(x_1, x_2, x_3)_{t=0} = (-1, -1, -1)$.

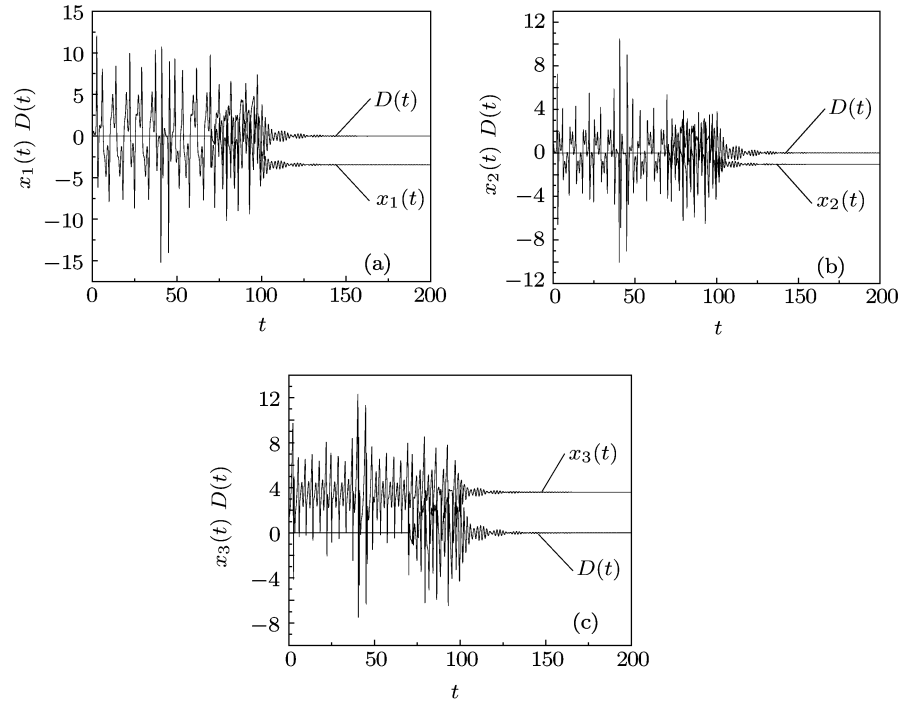


Fig. 4. The states of the controlled system (5) and the control system (6) response for $\tau = 2.62$ and $(x_1, x_2, x_3)_{t=0} = (-1, 1, 1)$.

Stability analysis of the delayed feedback systems is very difficult. Nevertheless, some general analytical results have been obtained.[13,14] It has been shown that the DFC can stabilize only a certain kind of periodic orbits characterized by a finite torsion. More precisely, the limitation is that any UPOs with an odd number of real Floquet multipliers (FMs) greater than unity can never be stabilized by the DFC. Numerical simulations have verified that the unstable saddle point E_0 possessing an odd number of real positive eigenvalues in uncontrolled system (1) cannot be stabilized anyway. Under the circumstances, an adaptive control method is proposed to overcome this limitation in the next section.

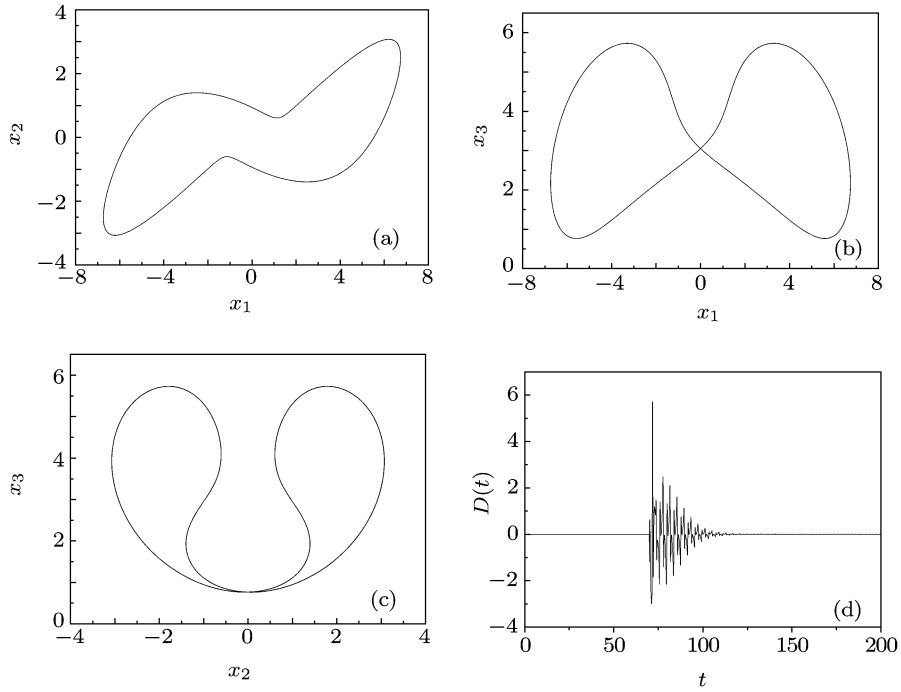


Fig. 5. The periodic trajectory of period-1 of the controlled system (5) for $\tau = 1.96$ and $(x_1, x_2, x_3)_{t=0} = (-1, -1, 1)$. Panels (a)–(c) show the periodic orbits to be stabilized in phase plane; panel (d) indicates $D(t)$ evolution with t.

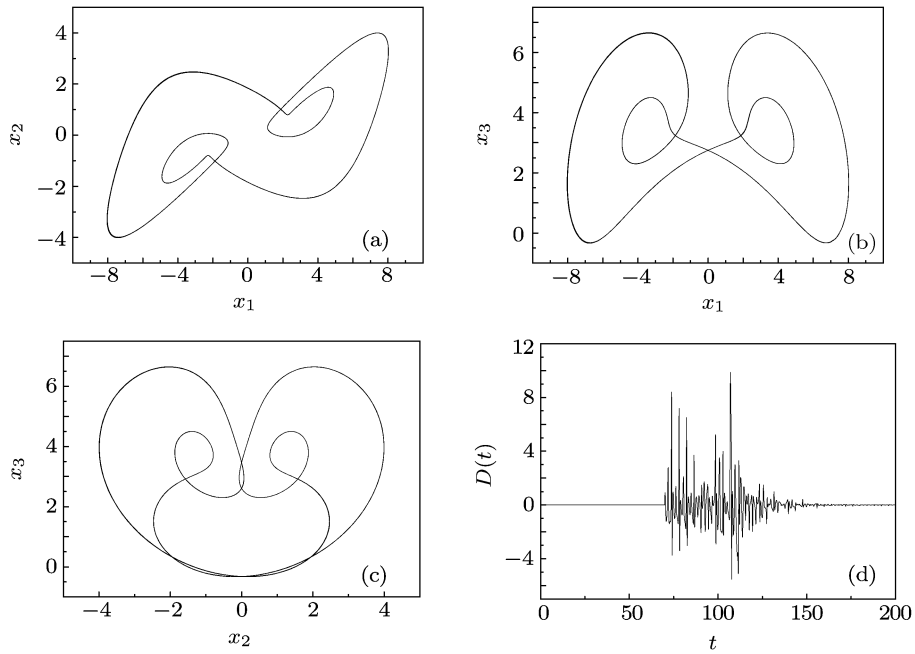


Fig. 6. The periodic trajectory of period-2 of the controlled system (5) for $\tau = 4.04$ and $(x_1, x_2, x_3)_{t=0} = (-1, -1, 1)$. Panels (a)–(c) show periodic orbits to be stabilized in phase plane; panel (d) indicates $D(t)$ evolution with t.

3.2. Adaptive control method

Our aim is to stabilize the chaotic system (1) to the unstable focus E_0, which the DFC fails to achieve due to its limitation. An adaptive control based on the LaSalle's invariance principle makes up for this shortcoming, and the detailed numerical proof and some interesting remarks on the results can be obtained in a series of papers.[15−17] In this section, the adaptive control is applied to system (1) to stabilize unstable fixed points.

Consider an n-dimensional system governed by the ordinary differential equation $\dot{x} = f(x)$, the controlled system with controlled perturbation u reads

$$\dot{x} = f(x) + u, \tag{7}$$

where u is an $n \times n$ matrix, constructed by a reference-free feedback perturbation that automatically locates and stabilizes the fixed point. Such a perturbation should vanish when the system settles at the fixed point. Here, according to Ref. [15], a closed-loop controller with variable feedback gain $k = k(t)$ is proposed as follows:

$$u = -k(x - w), \quad \dot{k} = \varepsilon(x - w)^2, \tag{8}$$

where $\varepsilon \in R_+^n$, and the variable feedback gain $k(t) \in R_+^n$ is a nondecreasing positive function which tends monotonically to its maximum value k^* when the desired asymptotically stable equilibrium state x^* is reached, $x \to x^*$, $k \to k^*$. The estimated position of the equilibrium state w is obtained from Ref. [16]

$$\dot{w} = \lambda(x - w), \tag{9}$$

where $w \in R^n$ and $\lambda \in R_+^n$. This property guarantees that for any $\lambda > 0$ the solution of Eq. (9) is bounded and moreover $w \to x^*$. The equations of controlled system are given by Eqs. (7), (8) and (9)[17]

$$\begin{aligned} &\dot{x} = f(x) - k(x - w), \quad \dot{w} = \lambda(x - w), \\ &\dot{k} = \varepsilon(x - w)^2. \end{aligned} \tag{10}$$

However, it was recognized by Pyragas that it could not stabilize the trivial saddle point with steady-state estimator $\lambda > 0$, but it could with estimator $\lambda < 0$.[16]

Generally, the dimension of the proposed controller is reduced instead of full state control. For instance, only one-dimensional controller is added to the third ordinary differential equations (1), as a result, a complete set of equations for the controlled coupled dynamos system reads

$$\begin{cases} \dot{x}_1 = -\mu x_1 + x_2(x_3 + \alpha), \\ \dot{x}_2 = -\mu x_2 + x_1(x_3 - \alpha), \\ \dot{x}_3 = x_3 - x_1 x_2 - k(x_3 - w), \\ \dot{w} = \lambda(x_3 - w), \quad \dot{k} = \varepsilon(x_3 - w)^2. \end{cases} \tag{11}$$

The controlled systems of the ordinary differential equations are integrated by using the fourth-order Runge–Kutta method in time steps of 0.01. The parameters α and μ are taken to be 2 and 3 respectively, i.e. $\alpha = 3$ and $\mu = 2$ to ensure chaotic behaviours in the absence of the control. The initial conditions $(x_1, x_2, x_3, k, w)_{t=0} = (1, 1, 1, 0, 0)$ are chosen in all simulations.

3.2.1. Stabilizing unstable saddle point E_0

Setting $\varepsilon = 0.2$, $\lambda = -0.2$, and turning the controller on at $t = 50$, equation (11) is stabilized at E_0. Figure 7 shows the saddle point stabilization.

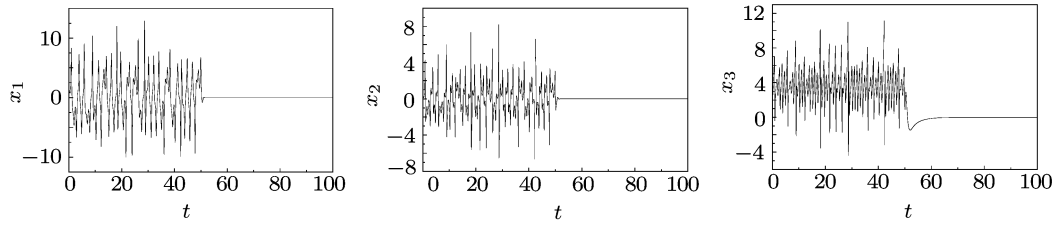


Fig. 7. Stabilization of unstable saddle point E_0 for the coupled dynamos system, with uncontrolled chaotic evolution $t \in [0, 50)$, controlled dynamics $t \in [50, 100)$, $\varepsilon = 0.2$, and $\lambda = -0.2$.

3.2.2. Stabilizing unstable focuses $E_1 \sim E_4$

If a controller is added to the first expression in Eq. (1), setting $\varepsilon = 0.2$, $\lambda = 0.2$, and turning the controller on at $t = 50$, the coupled system (1) is stabilized at $E_1(-1.045, 3.451, -3.606)$ and shown in Fig. 8. When the controller is turned on at $t = 46$, the coupled system (1) tends to another equilibrium state $E_2(1.045, -3.451, -3.606)$.

If a controller is added to the second expression in Eq. (1), setting $\varepsilon = 0.2$, $\lambda = 0.2$, and turning the controller on at $t = 47$, the system (1) is stabilized around $E_3(3.4508, 1.0448, 3.6056)$; When the controller is turned on at $t = 50$, the system (1) will be stabilized around $E_4(-3.4508, -1.0448, 3.6056)$.

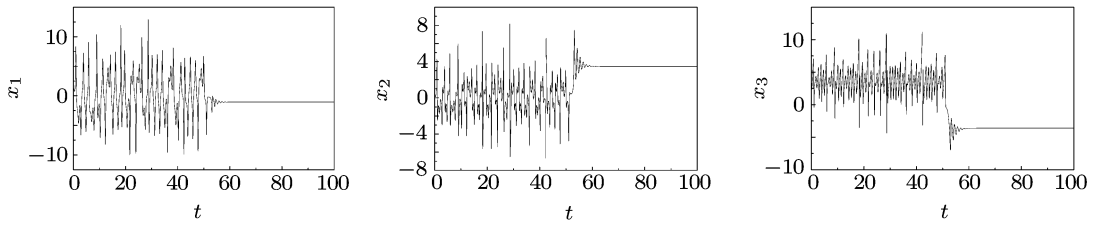


Fig. 8. Stabilization of unstable focus E_1 for the coupled dynamos system, with uncontrolled chaotic evolution $t \in [0, 50)$, controlled dynamics $t \in [50, 100)$. $\varepsilon = 0.2$, and $\lambda = 0.2$.

4. Conclusions

Two controlling chaos techniques which do not require any computer analytical knowledge of the system dynamics are appropriately applied to the dynamical system of coupled dynamos. The DFC method suppresses the chaotic behaviour of system (1) to unstable focuses and unstable periodic orbits. The adaptive control method has overcome the shortcoming of DFC, and it can stabilize the chaotic system (1) to not only an unstable saddle state, but also unstable equilibrium states effectively. The validity of these methods has been verified by numerical simulations.

References

[1] Ott E, Grebogi C and Yorke J A 1990 *Phys. Rev. Lett.* **64** 1196

[2] Braiman Y and Goldhirsch I 1991 *Phys. Rev. Lett.* **66** 2545

[3] Rajasekar S 1995 *Phys. Rev.* E **51** 775

[4] Ramesh M 1999 *Chaos, Solitons & Fractals* **10** 1473

[5] Liu Z H and Chen S G 1997 *Phys. Rev.* E **56** 168

[6] Liu Z H and Chen S G 1997 *Phys. Lett.* A **232** 55

[7] Wang X Y and Wu X J 2006 *Acta Phys. Sin.* **55** 5083 (in Chinese)

[8] Agiza H N 2002 *Chaos, Solitons & Fractals* **13** 341

[9] Agiza H N 2004 *Int. J. Mod. Phys.* C **15** 873

[10] Wang X Y 2003 *Chaos in the Complex Nonlinearity System* (Beijing: Electronics Industry Press) Chapt. 2 (in Chinese)

[11] Pyragas K 1992 *Phys. Lett.* A **170** 421

[12] Hu G, Xiao J H and Zheng Z G 2000 *Chaos Control* (Shanghai: Shanghai Scientific and Techonological Education Publishing House) p. 34

[13] Just W, Bernard T, Ostheimer M, Reibold E and Benner H 1997 *Phys. Rev. Lett.* **78** 203

[14] Nakajima H 1997 *Phys. Lett.* A **232** 207

[15] Huang D B 2006 *Phys. Rev.* E **73** 066204

[16] Pyragas K, Pyrags V, Kiss I Z and Hudson J L 2004 *Phys. Rev.* E **70** 026215

[17] Braun D J 2008 *Phys. Rev.* E **78** 016213